Available online at www.sciencedirect.com

ScienceDirect

Procedia Structural Integrity 35 (2022) 181–187

Structural Integrity Procedia

www.elsevier.com/locate/procedia

2nd International Workshop on Plasticity, Damage and Fracture of Engineering Materials

The influence of bi-layer metal-matrix composite coating on the strength of the coated material

Aleksandr Zemlianov[a,b,*], Ruslan Balokhonov[a], Varvara Romanova[a], Diana Gatiyatullina[a,b]

[a]*Institute of Strength Physics and Materials Science, Russian Academy of Sciences, pr. Akademicheskii 2/4, 634055 Tomsk, Russia*
[b]*National Research Tomsk State University, pr. Lenina 36, 634050 Tomsk, Russia*

Abstract

Deformation and fracture in aluminum with a bi-layer composite coating are studied numerically. Dynamic boundary-value problems in the plane-stress formulation are solved by the finite element method, using ABAQUS/Explicit. Isotropic elastoplastic and elastic-brittle constitutive models are used to simulate the mechanical response of the aluminum matrix and carbide ceramic particles, respectively. Microstructure of the composite coatings takes into account the complex shape of particles explicitly. To investigate the crack initiation and propagation in ceramic particles, a Huber type fracture criterion was chosen that takes into account the type of local stress state: bulk tension or compression. The influence of the arrangement of the coating layers on the fracture of ceramic particles and on the macroscopic strength of the coated materials is studied. Plastic strain localization, crack patterns and residual stress formation are numerically investigated during cooling followed by tension of the coated material.

Keywords: Numerical simulation, bi-layer coating, residual stresses, plastic strain localization, fracture

1. Introduction

Metal-matrix composites and coatings possessing high strength-to-weight ratio, wear resistance and durability are widely used in various industries (Zimmermann and Wang (2020); Arunachalam et al. (2018)). Because of a

* Corresponding author. Tel.: +7-961-863-6948; fax: +7 (3822) 49-25-76.
E-mail address: zem.aleks99@ispms.ru

10.1016/j.prostr.2021.12.063

complex hierarchically-organized microstructure of the composite and coated materials, their deformation behaviour is failed to be predicted within the traditional approaches used for conventional materials treated as quasi-homogeneous. Stress concentration arising in the region of inhomogeneities such as interfaces between the substrate and coating and matrix and particle induces plastic strain localization in the base material and surface layers. Physical mesomechanics deals with the investigation of deformation and fracture of composite materials and coatings (Panin et al. (1998)). The mechanical behaviour of the composites and coatings at various spatial scales with taking into account explicitly of internal boundaries should be considered to sufficiently study properties of composites.

There are different techniques to manufacture composite materials and coatings: stir casting (Panwar et al. (2020)), solid-state sintering (Furushima and Hyuga (2019)), cold spray deposition (Peat et. al (2017)), selective laser melting (Muvvala et al. (2017); Meng et al. (2006)) and others. It is also essential to apply proper machining conditions because they can affect the surface integrity (Liao et al. (2019)). One of the promising technologies for manufacturing and machining the composite coatings is laser deposition, which is used for improving the strength, corrosion resistance and microhardness of modified surface layers (Zhao et al. (2020); Fomin et al. 2020)). Residual stresses form during fabrication and deposition of coatings due to mismatch in thermal properties of the ceramics and metals (Faksa et al. (2019)). Problems concerned with the influence of residual stresses on the mechanical properties of composite materials are not completely solved yet. Different metal alloys and ceramic reinforcements are used as matrix and particle materials, respectively. The method of active screen plasma nitriding makes it possible to form a two-layer composite coating consisting of a part of the surface with particles of iron nitride and a lower part with particles of iron and aluminum nitrides (Taherkhani and Soltanieh (2020)). Multilayer coatings significantly improve the wear resistance of aluminum alloys (Zhang et al. (2020)) and exhibit excellent tribocorrosion resistance of the coated materials (Zhao et al. (2020)).

There are both experimental and numerical methods for examining the composites (Muvvala et al. (2018); Kadolkar et al. (2007); Balokhonov et al. (2021)). Experiments are rather expensive and time-consuming while computer-aided design of materials makes it possible to carry out scientific research calculations with high accuracy in describing microstructure of materials under study. Deformation behaviour of particle-reinforced metal matrix composites with the actual microstructure is analyzed by the finite element software (Chawla et al. (2006); Peng et al. (2020)). Numerical simulation is used to study the influence of properties of the compound materials, volume fraction of reinforcements in the coating on the deformation and fracture of the composites. An advantage of the numerical simulation is the possibility of varying one parameter, with the others being the same, which is difficultly realized during an experiment.

The influence of cooling-induced residual stresses on the fracture in composites was studied in (Balokhonov et al. (2021)), where the deformation of aluminum microvolume containing single ceramic particle was simulated. Single layer composite coating preliminary subjected to the stress relieving was considered in (Balokhonov et al. (2019); Balokhonov et al. (2020)). The novelty of the present study is to analyze the influence of the bi-layer coating reinforced by different ceramic particles on the deformation and fracture of the coated material, with the cooling-induced residual stresses being taken into account.

2. Methodology

In order to factor into the microstructure of the bi-layer coated material explicitly, SEM micrograph showing the cross section of the «aluminum-titanium carbide» coating produced by laser deposition was chosen (Fig. 1a). To construct the FE model the experimental image was simplified to take into account the prominent particles (Fig. 1b). The three-color pixel image was transformed to the spatial region of the coated material of the required size and discretized by regular rectilinear mesh containing 1300x800 square elements of CPS4R type (Fig. 1c,d). This orphan mesh written as an *.inp file was imported into ABAQUS software package. Isotropic elastic-plastic and elastic-brittle constitutive models describing the mechanical response of the aluminum matrix and ceramic particles, respectively, were developed and integrated into the ABAQUS/Explicit packager by the VUMAT user-defined subroutine. Plane stress boundary value problems on tension of the microstructure shown in Fig. 1c were solved from both initial zero and cooling-induced deformed states.

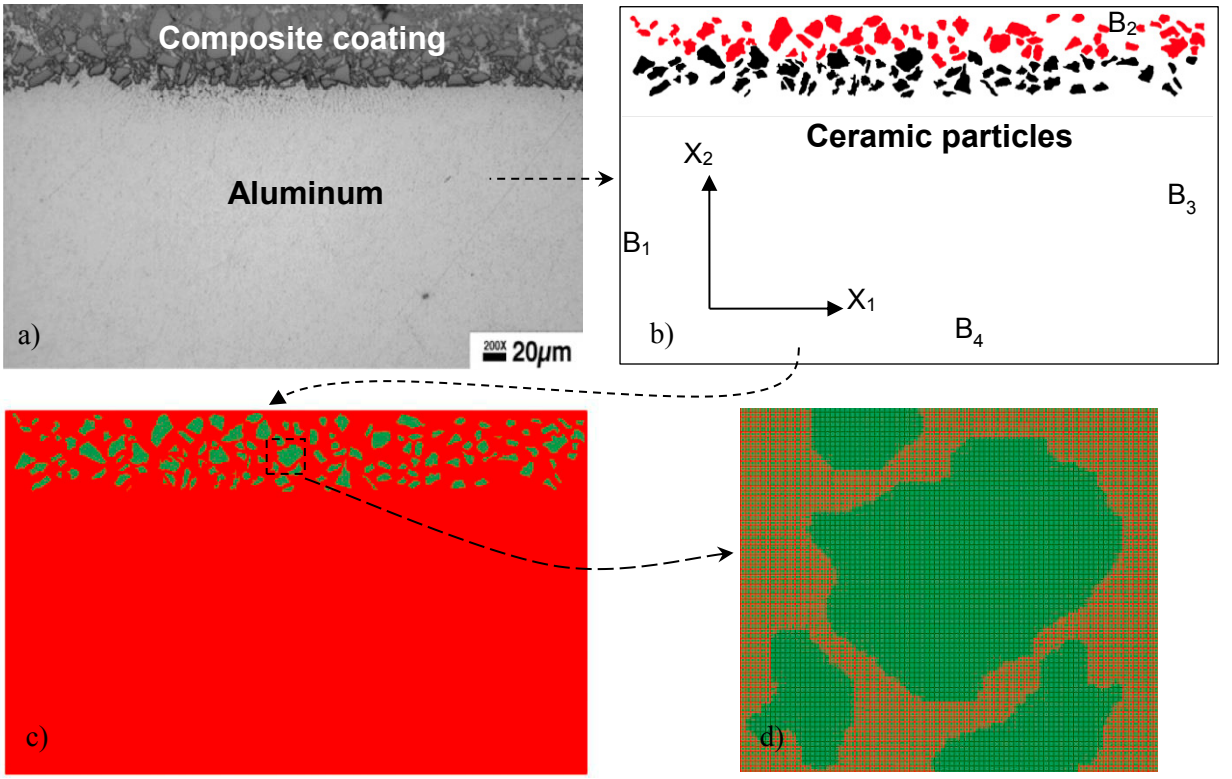

Fig. 1. Experimental image (a) and model structure of the bi-layer coated material (b), finite element discretization (c, d).

Preliminary cooling is simulated by the linear decrease of the temperature identical in the entire computational domain from 350 to 23 °C. Duhamel – Neumann's relations were used to take into account the thermal deformation of the materials:

$$\dot{\sigma}_{ij} = K(\dot{\varepsilon}_{kk} - 3\alpha\dot{T})\delta_{ij} + 2\mu(\dot{\varepsilon}_{ij} - \dot{\varepsilon}_{kk}\delta_{ij}/3 - \dot{\varepsilon}^{p}_{ij}) \tag{1}$$

where σ_{ij}, ε_{ij} and ε^{p}_{ij} are the tensors of stress, strain and plastic strain, δ_{ij} means the Kronecker delta, K and μ are the elastic bulk and shear moduli, α is the thermal expansion coefficient, T is the temperature, the dot denotes time derivative.

Associated plastic flow rule $\dot{\varepsilon}^{p}_{ij} = \lambda S_{ij}$ and the yield potential given by $\sigma_{eq} - f(\varepsilon^{p}_{eq}) = 0$ are used for description of plastic deformation in the matrix, where ε^{p}_{eq} and σ^{p}_{eq} are the equivalent accumulated plastic strain and stress.

Strain hardening is isotropic and given by the function

$$f(\varepsilon^{p}_{eq}) = \sigma_S - (\sigma_S - \sigma_{0,2}) \cdot \exp(-\varepsilon^{p}_{eq} / \varepsilon^{p}_{r}) \tag{2}$$

where σ_S and $\sigma_{0,2}$ are the ultimate and yield stresses, ε^{p}_{r} determines current value of the strain hardening.

Huber's type fracture criterion is sensitive for the sign of the local stress-strain state

$$\sigma_{eq} = \begin{cases} C_{ten}, \; if \; p < 0 \\ C_{com}, if \; p > 0 \end{cases} \tag{3}$$

where C_{ten}, C_{com} are the critical tensile and compressive strength values of ceramics, p is the pressure.

During cooling all B_1, B_2, B_3 and B_4 are free surfaces. Tension of the coated material in the X_1-direction is simulated by kinematic boundary conditions on the B_1 and B_3 surfaces, while B_2 and B_4 surfaces are free from loads.

Coating layers (Fig. 1b) composed of the Al6061T6 aluminum matrix reinforced by boron or tungsten carbide particles were arranged in two combinations: B_4C top layer – WC bottom layer and, vice versa, WC top layer – B_4C bottom layer. For the sake of generality, the composite coating, where both layers are reinforced by B_4C particles, is also included into consideration for comparison. Experimental mechanical properties of the aluminum alloy and reinforcing particles are shown in Table 1.

Table 1. Mechanical properties of the compound materials.

Material	ρ, g/cm^3	μ	K, GPa	σ_S, MPa	$\sigma_{0,2}$, MPa	α, 10^{-6} °C^{-1}	C_{ten}, GPa	C_{com}, GPa	ε^p_r, %
Al6061T6	2.7	26	66	332	234	22	-	-	9.5
B_4C	2.6	197	235	-	-	4.5	0.5	5	-
WC	15.6	260	370	-	-	5	0.37	5	-

3. Results and discussions

The results of numerical simulation are presented in Figures 2-4. Figure 2 shows a comparison of the stress states with and without preliminary cooling of the bi-layer coated material with «WC top layer - B_4C bottom layer» arrangement of the coating layers. Figure 3 shows the plastic strains in the matrix and particle cracking for varying arrangement of layers, with and without taking into account residual stresses. Figure 4 shows the calculated stress-strain curves corresponding to these cases.

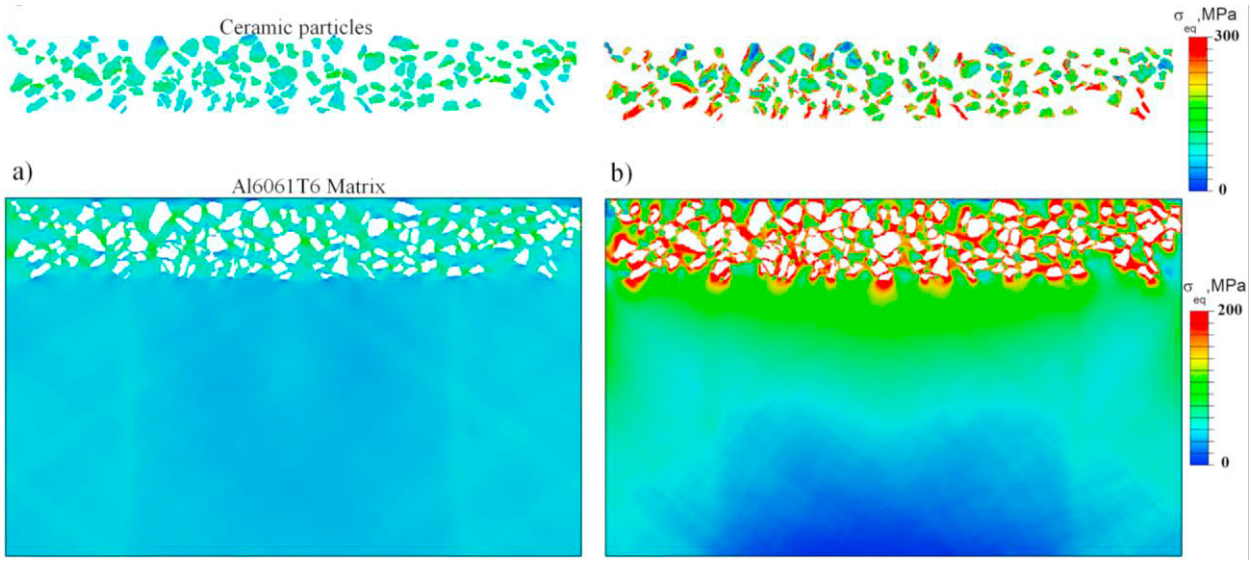

Fig. 2. Equivalent stress in bi-layer coated material with WC top – B_4C bottom coating layer arrangement under tension (a) and cooling followed by tension of the structure shown in Fig. 1b (b). Total strain of the coated material is 0.06%.

Under cooling of the coated material residual stress concentrations are formed in both the matrix and particles (Fig. 2b). It was shown that the regions of residual stresses are rounded regions localized in the matrix near the «matrix-particle» interfaces. High stresses concentrate near the interfacial asperities (Fig. 2b, Al6061T6 Matrix). Stresses in ceramic particles are higher than in the matrix (300 MPa versus 200 MPa maximum stresses), with the highest values being located near the coating-substrate interface (Fig. 2b, Ceramic particles). Fracture of particles begins even during cooling, i.e. fractured particles are observed even at a small tensile deformation of 0.06%.

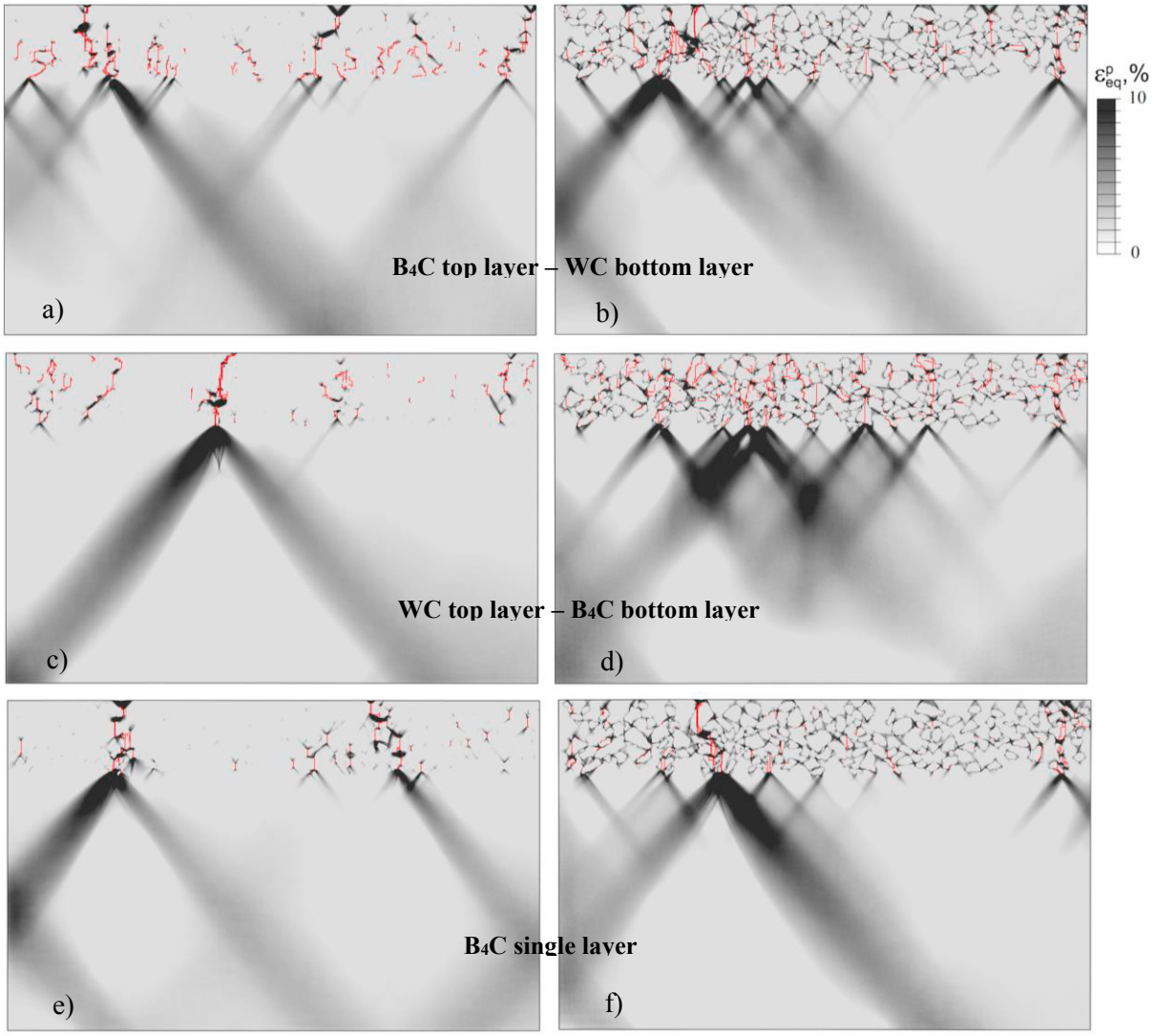

Fig. 3. Equivalent plastic strain under tension of the coated material with varying arrangement of the coating layers (a, c, e) and under cooling followed by tension (b, d, f). Fracture zones in ceramic particles are marked by red color. Total strain of the coated materials is 0.4%.

It was found that in the tungsten carbide particles forming the top coating layer cracks originate earlier than in the bottom layer boron carbide particles. This is because of the tungsten carbide has large elastic moduli K and μ, as well as lower tensile strength, compared to boron carbide. That is why the tensile strength of the tungsten carbide particles is reached earlier and they fracture occurs earlier than for the case of boron carbide ones. Residual stress concentrations induce plastic strains localized in the matrix around the particles, with the maximum values being located near the interfacial asperities and crack tips. The analysis of the plastic strain and crack patterns (Fig. 3) demonstrated that in the case of tension followed by cooling of the structure, many partially fractured particles are observed throughout the entire volume of the coating, while in the case of tension without preliminary cooling of the structure, a small number of particles are completely fractured. Weakly and strongly pronounced localized shear bands are formed, originating at the crack tips near the coating-substrate interface and propagating into the aluminium substrate at an angle of 45 degrees to the axis of loading. In the case of WC top - B_4C bottom coating layer arrangement the main crack is formed, which propagates to the free surface of the coating and to the coating-substrate interface.

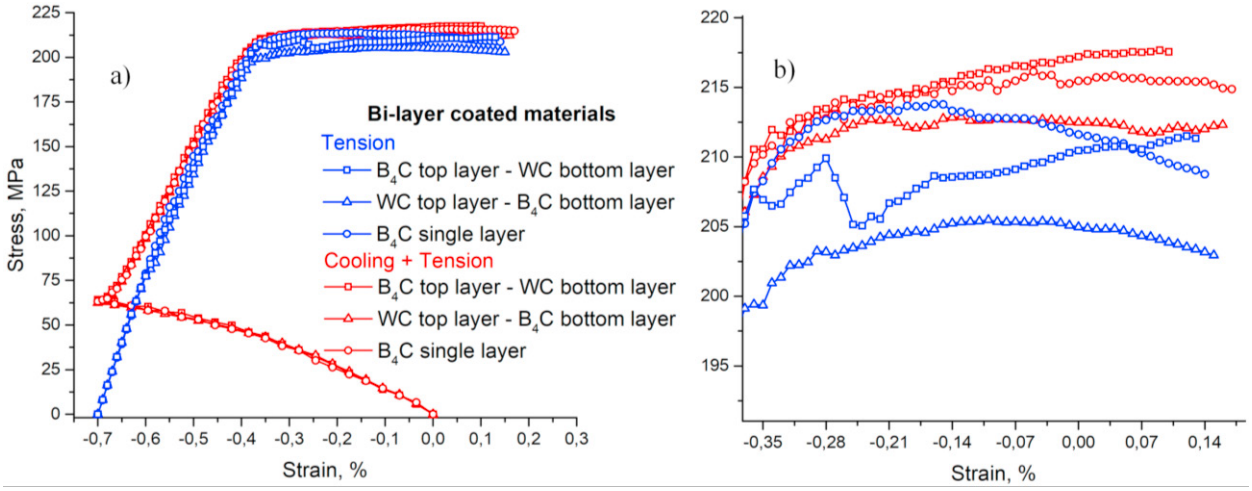

Fig. 4. Calculated stress-strain curves for varying arrangement of the coating layers, with and without preliminary cooling of the coated materials (a) and the scaled-up curves (b).

The macroscopic stress shown in Figure 4 is the equivalent stress averaged over the whole calculation region including substrate, matrix and particle materials, and the strain is the relative elongation of the region in the tension direction. For the comparative purpose the stress-strain curve for the case of cooling followed by tension of the structure starts from the strain of -0.7 % corresponding to the cooling-induced volumetric compression strain. The calculated stress-strain curves show that preliminary cooling increases the macroscopic strength of the coated material in all considered cases of the layer arrangement, with this increase being most pronounced in the case of the bi-layer coating (Fig. 4). Due to preliminary cooling of the coated material multiple cracking of carbide particles is observed, which prevents formation of the main crack (cf. Figs. 3c and d). Bi-layer coated material with B_4C top – WC bottom coating layer arrangement possesses the highest macroscopic strength because the intermediate layer with tungsten carbide particle serves as a damping sublayer reducing dangerous stress concentration in the coating.

4. Conclusions

Deformation and fracture in bi-layer metal-matrix composite coatings were numerically studied. The influence of the mechanical properties of the carbide particles composing the layers on the strength of the coated material was revealed. Analysis of the calculation results allows us to draw the following conclusions:

i. During cooling of the coated materials due to the difference in the coefficients of thermal expansion between the aluminum matrix and ceramic particles, residual stresses in the plastic matrix form concentrated circles, while in particles they occur near the interfacial asperities of highest curvature. This induces plastic flow in the aluminum matrix around the particles.

ii. Residual stresses are found to increase the strength of the coated materials in all considered cases of the coating layer arrangement. In the case of the bi-layer coating this increase is more pronounced than in the case «B_4C single layer», and the bi-layer coating with B_4C top – WC bottom coating layer arrangement possesses the highest macroscopic strength.

Acknowledgements

The work was supported by the Russian Science Foundation (grant No. 18-19-00273, https://rscf.ru/en/project/18-19-00273/). The fracture model described by Eq. (3) was developed according to the Government research assignment for ISPMS SB RAS, project FWRW-2021-0002.

References

Arunachalam, R., Krishnan, P.K., Muraliraja, R., 2018. A review on the production of metal matrix composites through stir casting–Furnace design, properties, challenges, and research opportunities. Journal of Manufacturing Processes 191, 33–45.

Balokhonov, R., Romanova, V., Schmauder, S., Emelianova, E., 2019. A numerical study of plastic strain localization and fracture across multiple spatial scales in materials with metal-matrix composite coatings. Theoretical and Applied Fracture Mechanics 101, 342-355.

Balokhonov, R., Romanova, V., Kulkov, A., 2020. Microstructure-based analysis of deformation and fracture in metal-matrix composite materials. Engineering Failure Analysis 110, 104412.

Balokhonov, R., Zemlianov, A., Romanova, V., Bakeev R., Evtushenko, E., 2021. Computational analysis of the influence of thermal residual stresses on the strength of metal-matrix composites. Procedia Structural Integrity 31, 58– 63.

Chawla, N., Sidhu, R.S., Ganesh, V.V., 2006. Three-dimensional visualization and microstructure-based modeling of deformation in particle-reinforced composites. Acta Materialia 54, 1541–1548.

Faksa, L., Daves, W., Klünsner, T., Maier, K., Antretter, T., Czettl, C., Ecker, W., 2019. Shot peening-induced plastic deformation of individual phases within a coated WC-Co hard metal composite material including stress-strain curves for WC as a function of temperature. Surface and Coatings Technology 380, 125026.

Fomin, V.M., Golyshev, A.A., Kosarev, V.F., Malikov, A.G., Orishich, A.M., and Filippov, A.A., 2020. Deposition of Cermet Coatings on the Basis of Ti, Ni, WC, and B4C by Cold Gas Dynamic Spraying with Subsequent Laser Irradiation. Physical Mesomechanics 23, 291-300.

Furushima, R., Hyuga, H., 2019. Fabrication of dense Al2O3-FeAl composites by using solid-state sintering. International Journal of Refractory Metals and Hard Materials 80, 292-298.

Kadolkar, P.B., Watkins, T.R., De Hosson, J.Th.M., Kooi, B.J., Dahotre, N.B., 2007. State of residual stress in laser-deposited ceramic composite coatings on aluminum alloys. Acta Materialia 55 (4), 1203-1214.

Liao, Z., Abdelhafeez, A., Li, H., Yang, Y., Diaz, O.G., Axinte D., 2019. State-of-the-art of surface integrity in machining of metal matrix composites. International Journal of Machine Tools and Manufacture 143, 63-91.

Meng, Q.W., Geng, L., Zhang, B.Y., 2006. Laser cladding of Ni-base composite coatings onto Ti–6Al–4V substrates with pre-placed B4C+NiCrBSi powders. Surface and Coatings Technology 200 (16–17), 4923–4928.

Muvvala G., Karmakar D.P., Nath A. K., 2017. Online assessment of TiC decomposition in laser cladding of metal matrix composite coating. Materials & Design 121, 310–320.

Muvvala, G., Karmakar, D.P., Nath, A.K., 2018. In-process detection of microstructural changes in laser cladding of in-situ Inconel 718/TiC metal matrix composite coating. Journal of Alloys and Compounds 740, 545-558.

Panin, V.E., Korotaev, A.D., Makarov, P.V., Kuznetsov V. M., 1998. Physical mesomechanics of materials. Russian Physics Journal 41, 856–884.

Panwar, N., Chauhan, A., Pali, H.S., Sharma, M.D., 2020. Fabrication of Aluminum 6061 Red-mud Composite using Stir Casting and Micro Structure Observation. Materials Today: Proceedings 21(4), 2014-2023.

Peat, T., Galloway, A., Toumpis, A., McNutt, P., Iqbal, N., 2017. The erosion performance of cold spray deposited metal matrix composite coatings with subsequent friction stir processing. Applied Surface Science 396, 1635–1648.

Peng, P., Gao, M., Guo, E., Kang, H., Xie H., Chen, Z., Wang, T., 2020. Deformation behavior and damage in B4Cp/6061Al composites: An actual 3D microstructure-based modeling. Materials Science and Engineering: A 781, 139169.

Taherkhani, K., Soltanieh, M., 2020. Spectroscopy study of composite coating created by a new method of active screen plasma nitriding on pure aluminum. Surface and Coatings Technology 393, 125820.

Zhang, F., Ding, Y., Yan, S., He, J., Yin, F., 2020. Microstructure evolution and mechanical performance of Cr-N/Al-Cr multilayer coatings produced by plasma nitriding Cr-coated Al alloy. Vacuum 180, 109540.

Zhao, C., Zhu, Y., Yuan, Z., Li, J., 2020. Structure and tribocorrosion behavior of Ti/TiN multilayer coatings in simulated body fluid by arc ion plating. Surface and Coatings Technology 403, 126399.

Zhao, Y., Lu, M., Fan, Z., Huang, S., Huang, H., 2020. Laser deposition of wear-resistant titanium oxynitride/titanium composite coatings on Ti-6Al-4V alloy. Applied Surface Science 531, 147212.

Zimmermann, N., Wang, P.H., 2020. A review of failure modes and fracture analysis of aircraft composite materials. Engineering Failure Analysis 115, 104692.